Submitted to ApJ, Part 1
Preprint typeset using LaTeX style emulateapj v. 20/04/00

arXiv:astro-ph/0008168v1 10 Aug 2000

# EVIDENCE FOR POLARIZED SYNCHROTRON COMPONENTS IN RADIO-OPTICAL ALIGNED QUASARS

Gary D. Schmidt

Steward Observatory, The University of Arizona, Tucson, AZ 85721

and

Paul S. Smith[1]

National Optical Astronomy Observatories, Kitt Peak National Observatory, Box 26732, Tucson, AZ 85726
*Submitted to ApJ, Part 1*

## ABSTRACT

A tendency for the axes of double-lobed radio quasars to be aligned with the electric vectors of optical polarization in the active galactic nuclei is well-known. However, the origin of the polarization and reason behind its correlation with radio morphology is not yet established. From accurate spectropolarimetry of 7 quasars which show this alignment effect, we find that the polarization is universally confined to the continuum, and not shared by the line emission or 3000 Å bump. Over the observed region $4000-8000$ Å, the spectral indices of polarized flux, $P \times F_\lambda$, are consistent with uniform polarization applied to the light of the big blue bump or with synchrotron emission. However, electron scattering from an optically-thick, geometrically-thin, accretion disk is well-known to give rise to a polarization position angle that is perpendicular to the disk axis. Optical synchrotron emission akin to that shown to exist in the miniblazar 3C 273 is a more attractive explanation, and supporting evidence can be found for some of the targets in the form of polarimetric variability over intervals of years. Properties of the most strongly-polarized radio-optical aligned quasars can be explained by misdirected blazar core components that have net polarizations of $P \sim 10\%$ and provide $\sim$10% of the total optical light.

*Subject headings:* galaxies: active — galaxies: jets — quasars: general — BL Lacertae objects: general — polarization

## 1. INTRODUCTION

The "Unified Scheme" for active galactic nuclei (AGN) has enjoyed remarkable success in explaining not only the spectroscopic and polarimetric properties of various classes of objects, but also their morphologies in the light of certain emission lines, the overall radio structure and spectra of quasars, and the existence of IR-luminous, but optically-faint AGN (e.g. Antonucci 1993; Cimatti et al. 1993; Capetti, Macchetto, & Lattanzi 1997; Hines et al. 1995). The idea relies on the presence of a nominally toroidal structure surrounding the central engine which obscures the compact object and broad-line region (BLR) for high-inclination sightlines. From such vantage points, the bright nuclear emission components are seen primarily in light which has become polarized by scattering off dust and/or electrons located above and below the polar openings of the torus. For these objects (e.g. Seyfert 2 galaxies, narrow-line radio galaxies, *IRAS* QSOs), extinction of the direct optical and near-IR continuum also increases the contrast of the emission from the more ubiquitous narrow-line region (NLR), earning their type-2 spectroscopic designation and resulting in extreme optical/far-IR colors.

By contrast, objects of type 1 are thought to be viewed through the toroidal hole, a perspective which provides the observer with a relatively unattenuated view of the central engine and BLR. Type-1 objects include the broad-line quasars, broad-line radio galaxies, and Seyfert 1 galaxies. When our sightline lies very near the axis of a relativistic jet emanating from the compact object, Doppler-boosted synchrotron emission from the jet dominates the spectrum and a highly variable and polarized blazar is observed. Though the model does not explain the essential difference between radio-loud and -quiet AGN, it successfully applies within each radio class.

Stockman, Angel, & Miley (1979) were the first to point out that the $E$-vector of optical polarization for quasars associated with double-lobe radio sources tends to be aligned with the radio source axis on the sky. This tendency toward "parallel" polarization was soon found to exist also among Seyfert 1 galaxies (Antonucci 1983) and radio galaxies (Antonucci 1982, 1984; Rudy et al. 1983), and to extend to radio structure at the milliarcsecond scale (Rusk & Seaquist 1985). Though interest in the radio-optical alignment was soon eclipsed by Antonucci's discovery (1983; see also Antonucci & Miller 1985) of very strong perpendicular polarization in some type-2 Seyfert galaxies, the result of Stockman et al. (1979) was early evidence for aspect-dependent classification of AGN.

There is no doubt that the dominant polarizing mechanism for most type-2 objects is small-particle scattering. Spectra of polarized flux ($P \times F_\lambda$) often show broad permitted lines that are not evident in the total flux spectrum but are characteristic of a classical emission-line QSO. In addition, the polarized continuum occasionally exhibits the "3000 Å bump", a pseudo-continuum from Fe II and Balmer free-bound emission arising within the

[1]Current address: Steward Observatory, The University of Arizona, Tucson, AZ 85721, psmith@as.arizona.edu

BLR (Grandi 1981; Wills, Netzer, & Wills 1985). The perpendicularity between the optical polarization $E$-vector and radio morphology is simply a result of the scatterers lying along the same general direction from the central source as the plasmons. In contrast, the polarization properties of radio-loud, non-blazar, type-1 AGN are not well-studied. Overall, the polarization of these objects rarely exceeds 2% (Stockman, Moore, & Angel 1984), so the sources are difficult to study in detail. The interpretation of weak polarization is also more ambiguous, since synchrotron emission, scattering in an extended halo or accretion disk, or even partial extinction by a medium of aligned dust grains are all potentially viable mechanisms (e.g., Stockman et al. 1979; Antonucci 1984). Discrimination among these possibilities requires spectropolarimetry of sufficient quality to measure the polarization of the emission lines *vs.* the continuum and to compare the continuum shape in polarized flux with that in total flux. Such a study is justified by the potential for new, qualitative information on the structure of the inner regions of QSOs and possibly on the salient distinction between radio-loud and -quiet objects.

## 2. OBSERVATIONS AND OBJECT SELECTION

In this paper we present the results of linear spectropolarimetry of 8 double-lobed quasars from the original Stockman et al. (1979) list which show alignment between the axis of radio emission and optical polarization. The data were obtained using the Steward Observatory 2.3 m Bok telescope and CCD Spectropolarimeter (Schmidt, Stockman, & Smith 1992). Wavelength coverage generally spans a single order of the low-resolution grating, $\lambda\lambda 4000-8000$, however on occasion a second tilt was used to include an important emission line. The data typically consist of $10-20$ observations from several epochs over the period $1995-1999$, each observation being the result of $\sim$20 min of integration in a $Q-U$ sequence of waveplate orientations. Entrance slits were $3''-4''$ width $\times\ 51''$ length, providing a spectral resolution of $\Delta\lambda \sim 12$ Å and ample real estate for sky subtraction. Basic properties of the targets and a summary of continuum polarization values measured at each epoch are listed in Tables 1 and 2, respectively. Only PKS 0405−123 showed such weak polarization in the initial observation that accurate spectropolarimetry was impractical[2]. With that lone exception, the new spectropolarimetric results are broadly consistent with "white-light" and filtered measurements from the 1970's and 1980's (e.g., Stockman, Moore, & Angel 1984; Berriman et al. 1990; Webb et al. 1993). In the spectropolarimetric results, the maximum position angle difference between the optical polarization and radio axis on either arcsecond (as) or milliarcsecond (mas) scales is $|\Delta\theta| = 28°$ (Table 3), so the new observations substantiate a long-term relationship between the two quantities.

For the 7 objects observed in detail, polarimetric variability was small, when present at all (see §4.2). Thus, the data for each object were coadded, weighting according to the statistical quality of each observation. The combined results are shown in Figures $1-7$, plotted as observed quantities *vs.* rest wavelength. Each figure portrays, from bottom to top, the total flux spectrum $F_\lambda$, the Stokes flux $q' \times F_\lambda$ for a coordinate system aligned with the overall position angle of polarization, the rotated Stokes parameter $q'$ in percent, and the electric-vector position angle $\theta$. For objects whose polarization position angles do not vary strongly with wavelength, such presentations are preferable to plots of the degree of polarization $P$ and polarized flux $P \times F_\lambda$ because they avoid having to apply statistical corrections for the positive bias of measurement errors on $P$. The final polarimetric signal-to-noise ratio for each object is $q'/\sigma_{q'} = 6-10$ per 20 Å wide bin, which is somewhat broader than a spectral resolution element.

The sample was chosen primarily to be tractable with a 2.3 m telescope. Generally, sources are optically bright, $V < 17$, and modestly polarized, $P \gtrsim 1\%$. All lie above a galactic latitude of 40° except 4C 34.47 ($b = 32°$). In any case, the lack of measurable polarization in the emission lines in any object (§3) rules out a significant interstellar component due to aligned grains in either the Milky Way or quasar host galaxy. The targets have total (core + lobes) radio luminosities $26 \lesssim \log(L_\nu(5\ \mathrm{GHz})) \lesssim 27$ (W Hz$^{-1}$) and core 5 GHz-to-optical flux ratios greater than 10 (Table 1). One of the most core-dominant of the radio sources, 4C 34.47, is also a known superluminal source (Barthel et al. 1989). Redshifts span the range $0.20 < z < 0.62$, so the H$\beta$+[O III] complex lies in the observed spectral range for all objects; lower-$z$ objects also provide H$\alpha$, and 3C 95 exhibits Mg II $\lambda$2800. In general, the emission-line components are very prominent in total flux.

Because targets were selected from a list already known to be polarized and with an orientation related to the radio structure, our sample is not well-suited in isolation for statistical evaluation of polarization properties *vs.* the predictions of a particular model (e.g., the Unified Scheme). Instead, our goal is to examine what can be learned about the polarizing mechanism in the aligned objects and possibly about the central regions of radio-loud quasars. Comparisons with spectropolarimetric compilations of other AGN may be informative but relevant selection criteria should be kept in mind. For example, Cohen et al. (1999) presented observations of 13 low-$z$ radio galaxies. That sample contains 8 narrow-line objects whose nuclei are presumably highly obscured; 6 of these reveal broad lines in polarized flux. Of the 5 broad-line radio galaxies, one was chosen by Cohen et al. because other observations suggested that it was heavily obscured. The remainder show no tendency toward alignment between optical polarization and radio structure, some contain large starlight components in their optical continua, and only one exhibits a true quasar-like spectrum. More recently, Malkan (2000) has made a study of several low-polarization QSOs of a variety of types, including 3 radio-loud objects.

A few of the targets observed here have been studied with spectropolarimetric techniques by others. Antonucci (1988) presented data of Miller and Goodrich on 4C 34.47 and Ton 202, PKS 0405−123 was studied by Antonucci et al. (1996), and Malkan (2000) discusses 4C 09.72. In none of these results do the emission lines or 3000 Å bump appear in polarized light, though the previous data on 3C 34.47 and Ton 202 are of low signal-to-noise ratio

[2]A broadband measurement made with a filter polarimeter and included in Table 2 confirms that this low polarization persisted as late as 1999 Oct.

and the polarization of PKS 0405−123 was very weak also when studied by Antonucci (1990 − 91; $P \approx 0.04\%$).

## 3. SPECTRA IN POLARIZED LIGHT

From inspection of Figures 1 − 7, it is clear that the following characteristics are universal among the objects studied:

1. a position angle of polarization that is essentially constant with wavelength,
2. a degree of polarization[3] that is diminished at the locations of broad and narrow emission lines, and
3. a reduction in polarization in the interval occupied by the 3000 Å bump: 2500 Å $\lesssim \lambda_{\rm em} \lesssim$ 5000 Å.

Malkan (2000) notes that the combination of all 3 of the above trends is found *only* in the radio-loud objects he studied. The results contradict a claim of Stockman et al. (1984) that the degree of polarization in a broad blue filtered bandpass generally exceeds that measured in the red. However, Stockman et al. point out that definite wavelength dependence was detected in only 2 of their objects. One is the $z = 2.23$, radio-quiet Broad Absorption Line QSO 1246−057 (e.g., Schmidt & Hines 1998), where the optical band examines a region well short of the 3000 Å bump. Evidence among the remainder of their sample is largely statistical in nature owing to large measurement uncertainties. Of the 4 objects which are in common with our spectropolarimetric sample, only Ton 202 showed a blue-red polarization difference exceeding the combined $1\sigma$ error bar: in that case, $P_B < P_R$, as we find.

Trends 2) and 3) above produce a spectrum of Stokes flux $q' \times F_\lambda$ which increases smoothly toward shorter wavelengths, showing no evidence of line emission. The confidence which can be placed on the claim of unpolarized lines varies from object to object according to the degree of polarization, data quality, and emission-line strength. We have used simple spectral synthesis techniques to estimate the fraction of the observed broad-line flux, $f_p$, which could share the polarization characteristics of the continuum, gauging the appearance of a polarized emission line in the models by eye. Because of the difficulty of setting a "continuum" level beneath the 3000 Å bump, we confine this test to the most prominent broad emission line in the spectrum: H$\alpha$, H$\beta$, or Mg II $\lambda$2800, as appropriate. The results are listed in Table 4 as $3\sigma$ upper limits to the polarized fraction of these features. Limits range from $f_p < 0.4$ for the H$\alpha$ line of 4C 34.47 to $f_p < 1.5$ for the weak H$\beta$ feature in 4C 09.72. Four of the 7 targets yield $3\sigma$ upper limits so low that only a portion of the line could be polarized like the continuum. This conclusion contrasts sharply with typical polarized type 2 sources, where broad lines generally appear *only* in polarized light, $f_p \gg 1$.

It should be pointed out that the above-quoted confidence levels are quite conservative: Several unpolarized emission features are present in most spectra, and statistical limits for the ensemble would be tighter than for the single brightest line. Furthermore, since the 3000 Å bump is thought to arise largely as gaseous emission within the BLR, the observed decline in polarization within the bump in each object is strong evidence for an unpolarized broad-line component. As an aside, we point out that many of the objects have sufficiently bright [O III] $\lambda\lambda$4959, 5007 lines to rule out the possibility that a significant portion of the narrow-line emission shares the polarization of the continuum.

Our results demonstrate that the polarization of the optical/radio aligned quasars studied here is a property solely of the continuum which underlies 3000 Å bump and is not shared by the emission lines. We have characterized the shape of this smoothly rising polarized continuum by a best-fit power law in Stokes flux $(q' \times F_\nu) \propto \nu^\alpha$. The resulting spectral indices $\alpha$ are listed in Table 4.

## 4. THE POLARIZING MECHANISM AND STRUCTURE OF THE NUCLEUS

The results presented above lead to several general conclusions regarding the polarizing mechanism in these radio-optical aligned quasars:

1. Each object is dominated by a single polarizing mechanism.
2. This mechanism acts entirely, or in large part, on the continuum of the object. If scattering is involved, the particles cannot lie substantially outside either of the emission-line regions. Electrons are possible scatterers, but considering that the BLR in objects of this luminosity may be as large as 1 pc in radius (Kaspi et al. 2000), dust particles may also be viable if the grains are entrained in a wind near the condensation radius (Kartje 1995).
3. The fact that the polarizing mechanism is aware of the radio axis on pc through Mpc scales implicates an origin that is related to the collimation of, or radiation by, the particle beam: i.e. the accretion disk or emission from the jet itself. These two alternatives are discussed in detail below.

### 4.1. *A Scattering Disk?*

It is popular to interpret the "big blue bump" which dominates the optical/UV portion of the spectral energy distribution of a typical AGN as emission from an accretion disk that surrounds the compact object. Though the shape of this bump is not a power-law over long spectral baselines, Francis et al. (1991) measured optical-near UV continuum slopes for a large number of radio-loud and -quiet QSOs, after correcting for the contributions of the Balmer-continuum and Fe II emission. The resulting histogram reveals that the great bulk of the objects falls in the range $-1.0 < \alpha < +0.3$, where $\alpha$ is the spectral index $F_\nu \propto \nu^\alpha$. It can be seen from comparison with Table 4 that this range also encompasses all of the slopes measured for the *polarized flux* spectra of the radio-optical aligned quasars studied here. The continuum shapes of these objects are therefore consistent with a spectrally-neutral polarizing mechanism applied to the light of the big blue bump.

[3]More accurately, the rotated Stokes parameter $q'$ (%)

Unfortunately, actual models of the polarization produced by physically-thin accretion disks are not as categoric (Koratkar & Blaes 1999; Koratkar et al. 1995; Antonucci et al. 1996). Briefly, simple optically-thick disk models imply a high opacity due to electron scattering, hence a substantial polarization when viewed at sufficiently large inclination, $i \gtrsim 45°$. This prediction is modified in spectral regions where the absorption opacity is also high, so strong polarimetric signatures are expected near bound-free edges. Spectropolarimetric observations have been made of a number of polarized QSOs in the region around the Lyman edge (e.g. Koratkar et al. 1995, 1998; Antonucci et al. 1996; Schmidt & Hines 1998). The data fail to show either the strong predicted continuum polarizations or the expected discontinuities. Moreover, scattering in an optically-thick, physically-thin disk results in a polarization $E$-vector which is *perpendicular* to the disk axis; the latter is thought to approximately coincide with the radio axis. This relationship is, of course, opposite to the trend observed among the radio-optical aligned quasars. Thus, simple thin disks seem to be ruled out on a number of accounts, a conclusion which seemed inevitable even in 1986 (Antonucci 1988). Suggested remedies to the situation include physically thick disks, winds, and additional scattering structures (see, e.g., Kartje 1995). Unfortunately, such complications reduce the predictability of models and as a result the utility of polarimetry as a diagnostic of the central structure of the nucleus.

A discussion of scattering disks in AGN would be incomplete without mentioning the case of OI 287. This object is an unusually strong narrow-line source[4] whose polarization is extremely high ($P \sim 8\%$), constant over time, and shows a position angle that is precisely aligned with the double-lobed radio structure (Rudy & Schmidt 1988). Like the radio-optical aligned quasars, the narrow emission lines are unpolarized. However, in OI 287 broad H$\beta$ and H$\gamma$ are evident in polarized light (Goodrich & Miller 1988; see also Antonucci, Kinney, & Hurt 1993), a fact which motivated a model involving obscuration and scattering of light originating in the central source and BLR by a physically (and optically?) thin disk that is viewed very nearly edge-on. While OI 287 demonstrates the feasibility of thin scattering disks resulting in strong parallel polarizations, its overwhelming narrow-line spectrum and polarized broad lines indicate that the source is viewed at a high inclination and may well be the product of a polarizing mechanism unrelated to that dominating the objects studied here.

### 4.2. *Synchrotron Alternatives*

Synchrotron emission is a well-known source of optical continuum and polarization in certain classes of AGN. It originates both from resolved, kpc-scale jet features such as those which emanate from several radio-loud AGN, and from variable components in the spectral energy distributions of blazars. The latter presumably also arise in small-scale jet structures which in the Unified Scheme (e.g. Antonucci 1993) are Doppler-boosted when a relativistic particle beam is viewed from near the axis of ejection. Recall that in the Unified Scheme, broad-line quasars are seen from a sufficiently small inclination that the torus does not intercept sightlines to the nucleus ($i \lesssim 45°$), so a weak optical synchrotron component from the relativistic jet would not be a great surprise.

With the exception of the enormous jet of 3C 273, the resolved optical jets associated with local AGN have projected lengths of a few kpc (e.g., Scarpa et al. 1999). At a distance typical of the sources in Table 1, they would subtend $<1''$ on the sky and be very difficult to discern against the bright nuclear source. Both well-studied local examples – M87 and 3C 273 – show superluminal motion (Biretta & Meisenheimer 1993; Unwin et al. 1985 and references therein) and have been mapped at $\lesssim 1''$ resolution in spectral index and polarization (Perlman et al. 1999; Conway & Röser 1993). The optical jets are not only associated with radio counterparts but are aligned with radio structure on the mas scale as well as with the giant lobes. The jets of both M87 and 3C 273 exhibit optical $E$-vectors of polarization that are generally perpendicular to the projected jet axes in the inner regions ($B$-fields parallel to the jets), flipping by $\sim 90°$ in knots that are presumed to be the sites of shocks. As a result, the polarization of each jet summed over its entire length is modest ($P \lesssim 10\%$). Finally, optical spectral indices measured for the local jet sources are: M87, $\alpha \approx -0.65$ independent of location (Biretta & Meisenheimer 1993) and 3C 273, $-1.7 < \alpha < -0.8$ (Conway & Röser 1993). Radio-optical spectral indices of jets associated with PKS 0521−365, 3C 371, and PKS 2201+044 measure $\alpha_{\rm RO} \approx -0.8$ (Scarpa et al. 1999). These slopes compare well with the spectral indices of polarized flux for the targets studied here ($-1.1 \lesssim \alpha \lesssim -0.8$), except for 4C 34.47 ($\alpha \approx +0.1$; Figure 6 and Table 4).

The difficulty with the hypothesis that kpc-scale jets are the origin of polarization in the radio-optical aligned quasars is the low optical luminosities of known examples. Monochromatic values at $V$ summed over the lengths of the above-mentioned jets range from $L_{5500} \sim 6 \times 10^{35}$ ergs s$^{-1}$ Å$^{-1}$ for PKS 2201+044 to $\sim 7 \times 10^{38}$ ergs s$^{-1}$ Å$^{-1}$ for 3C 273[5]. These must be compared with the optical luminosity for a typical quasar from our sample ($V \approx 16$, $z \approx 0.35$) of $\sim 10^{42}$ ergs s$^{-1}$ Å$^{-1}$. Indeed, if the jet of 3C 273 were unresolved from the central source, it would give rise to a net optical polarization for the quasar of $P < 0.01\%$. Of course, it is possible that our selection of the most highly polarized quasars has also identified sources with unusually bright or polarized optical jets. However, the structures would have to be at least an order of magnitude more luminous than any local example and be uniformly polarized near the synchrotron maximum of $P \approx 70\%$ to yield the levels of polarization listed in Table 2.

More promising is the possibility of synchrotron emission from a misdirected blazar core component or an intrinsically weak end-on blazar. Except for 4C 34.47, the spectral indices of polarized flux of the radio-optical aligned quasars are consistent with the optical-near UV range measured for blazars (e.g. Landau et al. 1986), and a synchrotron component with moderately strong polarization ($P \sim 10\%$) that provides $\lesssim 10\%$ of the total con-

[4]Indeed, Antonucci et al. (1993) term it a Quasar 2.

[5]Cosmological parameters $H_0 = 75$ km s$^{-1}$ Mpc$^{-1}$ and $q_0 = \frac{1}{2}$ are assumed.

tinuum flux would account for the observed levels of polarization. The canonical benchmark for a highly-polarized quasar has been that the broadband optical polarization exceed $P = 3\%$ (e.g. Moore & Stockman 1981; Stockman et al. 1984; Wills et al. 1992). This criterion was based on the bimodal distribution of polarization observed among survey QSOs (Stockman 1978), a fact that suggested different polarizing mechanisms dominate in the two regimes. While it is true that quasars exceeding the 3% limit are very likely to show blazar-like properties, it is quite possible – indeed probable – that some weakly-polarized objects also contain feeble synchrotron components. Remarkably, the best example of a miniblazar is found in the prototypical emission-line quasar 3C 273 (Impey, Malkan, & Tapia 1989; Wills 1989). Highly variable in polarization but generally showing $P < 0.5\%$ at optical wavelengths, 3C 273 occasionally exhibits "flares" when the $I$-band polarization reaches 2% (Courvoisier et al. 1988; Impey et al. 1989; de Diego et al. 1992). Dilution by the 3000 Å and big blue bumps cause the degree of polarization to decline toward the blue and the emission lines are measured to be patently unpolarized (Smith, Schmidt, & Allen 1993; de Diego et al. 1992). From the same observations, it was found that the spectrum of polarized flux in the optical-UV is rather steep, $\alpha < -1.5$, and variable. Though the polarization position angle has been measured to vary through a range of at least 120°, values tend to cluster around a mean of $\theta \sim 60°$ (Impey et al. 1989), close to the $\theta = 43°$ orientation of the resolved jet and radio lobes. Thus, 3C 273 could well be classified as a quasar that shows alignment between its optical polarization and radio structure. A lower-luminosity analog is the type-1 Seyfert galaxy NGC 4151, which contains a variable continuum component that has been studied extensively throughout the electromagnetic spectrum and whose optical polarization lies within ∼10° of the axis of the two-sided arcsecond-scale radio jet (e.g., Schmidt & Miller 1980; Pedlar et al. 1993).

The classic test for blazar activity is variability. The polarimetric data available to us (Stockman et al. 1984; Webb et al. 1993) coupled with the observations summarized in Table 2 provide 5−10 epochs of broadband measurements for each object in our sample. The data span a total time base of typically 20 yr and sample intervals of about a month to a decade. A simple $\chi^2$ analysis of the measurements uncovers a few interesting cases. Foremost is the aforementioned PKS 0405−12, which was found to have $P \geq 0.50\%$ on two occasions by Stockman et al. (1984) but has always been measured at <0.30% since. The position angle of polarization, which is probably a more robust indicator since it is not as sensitive to differences in waveband or to variable dilution, shows values for this quasar that range over nearly the entire compass. Even in 1978−80, when the source was comparatively strongly polarized, a range of $\Delta\theta = 24°$ was measured. Unfortunately, PKS 0405−12 has been so weakly polarized of late that accurate spectropolarimetry has been impossible (see also Antonucci et al. 1996).

Three other targets from our sample show some evidence for polarimetric variability. The $\chi^2$ index for the position angle measurements of Ton 202, 4C 37.43, and 4C 09.72 are 35, 23, 23 for 9, 4, 6 degrees of freedom, respectively, corresponding to probabilities of chance occurrence of $10^{-4} - 10^{-3}$. The range of variation is not great, amounting to $\Delta\theta \sim 30°$ for 4C 09.72 and 4C 37.43 and ∼20° for Ton 202. However, these cases are unlikely to be statistical flukes, since measurements for B2 1208+32 and 4C 34.47, acquired to similar accuracy with the same instruments and over similar baselines, cover a total span in $\theta$ of just 12° and 8°, respectively, and yield $\chi^2_\theta = 3$ for 6 degrees of freedom for each object. Unfortunately, the detection of variability requires high relative precision in the measurements, and available data for these quasars are not of uniformly high quality. If 3C 273 were not virtually on our doorstep, it is likely that its miniblazar source would remain undiscovered even today.

While polarimetric variability may be a sufficient condition for identifying the synchrotron mechanism, it may not be necessary. Even the most active blazars often exhibit "preferred" polarization position angles in extensive monitoring campaigns (e.g. Angel et al. 1978), suggesting a systemic axis possibly associated with that of the accretion disk. The synchrotron components proposed here would be much more stable than those of classical blazars, but this is qualitatively consistent with jets viewed at larger angles to the ejection axis. A strong link between the existence of a beamed optical component and core-dominant radio structure is well-established (e.g. Impey & Tapia 1988; Wills et al. 1992), and strong optical polarization is almost always seen in superluminal sources. It is therefore interesting that the most core-dominant of our targets, 4C 34.47, with $\log(F_{\rm core}/F_{\rm tot}) \approx -0.3$, lies in the range where a majority of sources would show high polarization (Impey et al. 1989). 4C 34.47 has also shown superluminal motion with the rather modest apparent speed of $\beta_{\rm app} \sim 3$ (Barthel et al. 1989). The projected expansion axis was oriented at $\theta = 167°$, very nearly aligned with the large-scale structure and only 19° from the optical polarization position angle. A simple beaming model suggests that the jet lies within 44° of the line of sight. Once again we draw a parallel to 3C 273, which is a superluminal source showing $5 \lesssim \beta_{\rm app} \lesssim 8$ and a corresponding viewing angle of <20° (Unwin et al. 1985). On the other hand, the unusually flat spectral index of polarized flux measured for 4C 34.47 would require a miniblazar source of unprecedented properties – one with a remarkably flat synchrotron spectrum and/or strong intrinsic wavelength dependence to its polarization.

## 5. DISCUSSION

The preceding sections present modest evidence that the optical polarization of radio quasars may be due largely to synchrotron emission from misdirected or intrinsically weak blazar core components. Because this hypothesis implies the presence of an exposed relativistic jet, and such jets are presumably absent in radio-quiet objects, it might be expected that radio quasars would be overrepresented among AGN with small but significant polarization in large-scale surveys. Of course, this implies equality between the classes with respect to other variables (dust content, orientation, starlight fraction, etc.). In their statistical analysis of the polarization of Palomar-Green (PG) QSOs, Berriman et al. (1990) discriminated explicitly according to radio properties. Their Figure 3 indeed shows that a significantly larger fraction (5:17) of radio-loud objects (those with $F_\nu(5\ {\rm GHz})/F_\nu({\rm opt}) > 25$)

are found with $P > 1\%$ than for the radio-quiet sample (9:80). Four of the radio-luminous PG sources are spectropolarimetric targets studied here. However, Berriman et al.'s breakdown according to radio core dominance showed no correlation within either the radio-loud or -quiet samples, and a major conclusion of that paper was the general lack of evidence for synchrotron components in the sources studied. The techniques applied by Berriman et al. (1990) were effective at discriminating against highly polarized AGN of either the scattering or blazar variety, but since the PG catalog is derived from optical selection criteria, the radio-loud subsample is small. The criteria used – polarimetric variability and the dependence of $P(\%)$ on radio core dominance and optical color – were inefficient at identifying weak nonthermal components when the observable itself was known to a typical accuracy of only $\sigma_P \sim 0.2\%$ ($P/\sigma_P \lesssim 5$). Indeed, the prototype miniblazar, 3C 273, fails to stand out in any of the diagnostic tests made by Berriman et al., despite the fact that it is a particularly bright and easily measured member of the PG catalog. The weak polarization that is observed at wavelengths as long as 2 $\mu$m in 3C 273 as well as for 3 of the spectropolarimetric targets studied here (Sitko & Zhu 1991) indicates that the putative synchrotron components would also be minor contributors to the observed flux in the infrared. Unfortunately, none of the sources studied here were detected by *IRAS*, but they would make interesting *SIRTF* targets. Detailed spectral energy distributions, plus comprehensive polarimetric monitoring and additional investigations of the type carried out here, may be required to confirm the existence and prevalence of synchrotron components as significant sources to the optical continua of quasars.

Special thanks go to D. Hines, M. Malkan, and the referee, R. Antonucci, for illuminating discussions and critical readings of the manuscript. Support for this work was provided by NSF grants AST 91-14087 and AST 97-30792 and by the Director of KPNO.

REFERENCES

Angel, J.R.P., et al. 1978, in Pittsburgh Conference on BL Lac Objects, ed. A.M. Wolfe (Pittsburgh: University of Pittsburgh), 117
Antonucci, R.R.J. 1982, Nature, 299, 605
_____. 1983, Nature, 303, 158
_____. 1984, ApJ, 278, 499
_____. 1988 in Supermassive Black Holes, ed. M. Kafatos (Cambridge: Cambridge Univ. Press), 26
_____. 1993, ARA&A, 31, 473
Antonucci, R., Geller, R., Goodrich, R.W., & Miller, J.S. 1996, ApJ, 472, 502
Antonucci, R., Kinney, A.L., & Hurt, T. 1993, ApJ, 414, 506
Antonucci, R.R.J., & Miller, J.S. 1985, ApJ, 297, 621
Barthel, P.D., Hooimeyer, J.R., Schilizzi, R.T., Miley, G.K., & Preuss, E. 1989, ApJ, 336, 601
Berriman, G., Schmidt, G.D., West, S.C., & Stockman, H.S. 1990, ApJS, 74, 869
Biretta, J.A., & Meisenheimer, K. 1993, in Jets in Extragalactic Radio Sources, eds. H.-J. Röser & K. Meisenheimer (Berlin: Springer-Verlag), 159
Capetti, A., Macchetto, F.D., & Lattanzi, M.G. 1997, ApJ, 476, L67
Cimatti, A., di Serego Alighieri, S., Fosbury, R.A.E., Salvati, M., & Taylor, D. 1993, MNRAS, 264, 421
Cohen, M.H., Ogle, P.M., Tran, H.D., Goodrich, R.W., & Miller, J.S. 1999, AJ, 118, 1963
Conway, R.G., & Röser, H.-J. 1993, in Jets in Extragalactic Radio Sources, eds. H.-J. Röser & K. Meisenheimer (Berlin: Springer-Verlag), 199
Courvoisier, T.J.-L., Robson, E., Hughes, D., Blecha, A., Bouchet, Pl, Krisciunas, K., & Schwarz, H. 1988, Nature, 335, 330
de Diego, J.A., Pérez, E., Kidger, M.R., & Takalo, L.O. 1992, ApJ, 396, L19
Fanti, C., Fanti, R., Formiggini, L, Lari, C., & Padrielli, L. 1977, A&AS, 28, 351
Francis, P., Hewett, P.C., Foltz, C.B., Chaffee, F.H., Weymann, R.J., & Morris, S.L. 1991, ApJ, 373, 465
Goodrich, R.W., & Miller, J.S. 1988, ApJ, 331, 332
Grandi, S.A. 1981, ApJ, 251, 451
Hines, D., Schmidt, G.D., Smith, P.S., Cutri, R., & Low, F.J. 1995, ApJ, 450, L1
Impey, C.D., Malkan, M.A., & Tapia, S. 1989, ApJ, 347, 96
Impey, C.D., & Tapia, S. 1988, ApJ, 333, 666
Kaspi, S., Smith, P.S., Netzer, H., Maoz, D., Jannuzi, B.T., & Giveon, U. 2000, ApJ, in press
Kartje, J.F. 1995, ApJ, 452, 565
Kellerman, K.I., Sramek, R.A., Schmidt, M., Green, R.F., & Shaffer, D.B. 1994, AJ, 108, 1163
Koratkar, A., Antonucci, R.R.J., Goodrich, R.W., Bushouse, H., & Kinney, A.L. 1995, ApJ, 450, 501
Koratkar, A., Antonucci, R.R.J., Goodrich, R., & Storrs, A. 1998, ApJ, 503, 599
Koratkar, A., & Blaes, O. 1999, PASP, 111, 1
Landau, R. et al. 1986, ApJ, 308, 78
Malkan, M.A. 2000, private communication
Moore, R.L., & Stockman, H.S. 1981, ApJ, 243, 60
Pedlar, A., Kukula, M.J., Longley, D.P.T., Muxlow, T.W.B., Axon, D.J., Baum, S., O'Dea, C., & Unger, S.W. MNRAS, 263, 471
Perlman, E.S., Biretta, J.A., Zhou, F., Sparks, W.B., & Macchetto, F.D. 1999, AJ, 117, 2185
Price, R., Gower, A.C., Hutchings, J.B., Talon, S., Duncan, D., & Ross, G. 1993, ApJS, 86, 365
Rudy, R.J., & Schmidt, G.D. 1988, ApJ, 331, 325
Rudy, R.J., Schmidt, G.D., Stockman, H.S., & Moore, R.L. 1983, ApJ, 271, 59
Rusk, R., & Seaquist, E.R. 1985, AJ, 90, 30
Scarpa, R., Urry, C.M., Falomo, R., & Treves, A. 1999, ApJ, 526, 643
Schmidt, G.D., & Hines, D.C. 1999, ApJ, 512, 125
Schmidt, G.D., & Miller, J.S. 1980, ApJ, 240, 759
Schmidt, G.D., Stockman, H.S., & Smith, 1992, ApJ, 398, L57
Sitko, M.L., & Zhu, Y. 1991, ApJ, 369, 106
Smith, P.S., Schmidt, G.D., & Allen, R.G. 1993, ApJ, 409, 604
Stockman, H.S. 1978, in Pittsburgh Conference on BL Lac Objects, ed. A.M. Wolfe (Pittsburgh: University of Pittsburgh), 149
Stockman, H.S., Angel, J.R.P., & Miley, G.K. 1979, ApJ, 227, L55
Stockman, H.S., Moore, R.L., & Angel, J.R.P. 1984, ApJ, 279, 485
Unwin, S.C., Cohen, M.H., Biretta, J., Pearson, T.J., Seielstad, G.A., Walker, R.C., Simon, R.S., & Linfield, R.P. 1985, ApJ, 289, 109
Webb, W., Malkan, M., Schmidt, G.D., & Impey, C.D. 1993, ApJ, 419, 494
Wills, B.J. 1989, in BL Lac Objects, eds. L. Maraschi, T. Maccacaro, & M.-H. Ulrich (Berlin: Springer), 109
Wills, B.J., & Browne, I.W.A. 1986, ApJ, 302, 56
Wills, B.J., Netzer, H., & Wills, D. 1985, ApJ, 288, 94
Wills, B.J., Wills, D., Breger, M., Antonucci, R.R.J., & Barvainis, R. 1992, ApJ, 398, 454

TABLE 1
OBJECT LIST

| Quasar | Coord. | $z$ | $V$ | $\log(L_\nu(5\ \mathrm{GHz}))^{a}$ (W $\mathrm{Hz}^{-1}$) | $\log R^{b}$ | $F_\nu(5\ \mathrm{GHz})/\mathrm{F}_\nu(\mathrm{opt})$ (core only) |
|---|---|---|---|---|---|---|
| 3C 95 | 0349−146 | 0.616 | 16.2 | 26.9 | −1.68 | 13 |
| PKS 0405−12 | 0405−123 | 0.574 | 15.8 | 27.2 | −0.23 | 384 |
| B2 1208+32 | 1208+322 | 0.388 | 16.0 | 25.7 | ··· | ··· |
| Ton 202 | 1425+267 | 0.362 | 15.7 | 25.6 | −0.40 | 19 |
| 4C 37.43 | 1512+370 | 0.371 | 15.5 | 26.0 | −0.71 | 24 |
| 3C 323.1 | 1545+210 | 0.264 | 16.7 | 26.0 | −1.32 | 41 |
| 4C 34.47 | 1721+343 | 0.206 | 16.5 | 25.8 | +0.06 | 353 |
| 4C 09.72 | 2308+098 | 0.432 | 16.0 | 26.1 | −0.78 | 28 |

[a]Total (core + lobe) luminosity computed using $H_0 = 75$ km $\mathrm{s}^{-1}$ $\mathrm{Mpc}^{-1}$, $q_0 = \frac{1}{2}$.

[b]Core-to-lobe flux ratio at 5 GHz, from Wills & Browne (1986).

TABLE 2
SPECTROPOLARIMETRY LOG

| Quasar | Epoch | # obs[a] | $P^{b}$ | $\theta^{b}$ |
|---|---|---|---|---|
| 3C 95 | 1995 Nov | 7 | $0.97 \pm 0.06\%$ | $175^\circ \pm 2^\circ$ |
| | 1996 Dec | 12 | $0.73 \pm 0.05\%$ | $177^\circ \pm 2^\circ$ |
| | 1999 Oct | 2 | $0.55 \pm 0.18\%$ | $178^\circ \pm 10^\circ$ |
| PKS 0405−12 | 1995 Nov | 1 | $0.27 \pm 0.19\%$ | $124^\circ \pm 20^\circ$ |
| | 1999 Oct[c] | 1 | $0.17 \pm 0.14\%$ | $90^\circ \pm 25^\circ$ |
| B2 1208+32 | 1996 Mar | 6 | $1.14 \pm 0.08\%$ | $18^\circ \pm 2^\circ$ |
| | 1996 Jun | 1 | $1.32 \pm 0.25\%$ | $14^\circ \pm 6^\circ$ |
| | 1996 Dec | 6 | $1.05 \pm 0.05\%$ | $17^\circ \pm 2^\circ$ |
| | 1997 Dec | 2 | $0.65 \pm 0.27\%$ | $15^\circ \pm 12^\circ$ |
| Ton 202 | 1996 Mar | 2 | $1.62 \pm 0.15\%$ | $67^\circ \pm 3^\circ$ |
| | 1996 Jun | 4 | $1.85 \pm 0.12\%$ | $64^\circ \pm 2^\circ$ |
| | 1997 Apr | 2 | $1.40 \pm 0.16\%$ | $69^\circ \pm 3^\circ$ |
| | 1997 Dec | 2 | $1.88 \pm 0.26\%$ | $75^\circ \pm 4^\circ$ |
| | 1998 Apr | 3 | $1.67 \pm 0.18\%$ | $69^\circ \pm 3^\circ$ |
| | 1999 May | 2 | $1.97 \pm 0.09\%$ | $74^\circ \pm 2^\circ$ |
| 4C 37.43 | 1996 May | 7 | $1.24 \pm 0.04\%$ | $101^\circ \pm 2^\circ$ |
| | 1999 May | 3 | $1.26 \pm 0.09\%$ | $100^\circ \pm 2^\circ$ |
| 3C 323.1 | 1996 Jun | 5 | $1.35 \pm 0.04\%$ | $23^\circ \pm 2^\circ$ |
| | 1998 Apr | 5 | $1.72 \pm 0.14\%$ | $20^\circ \pm 3^\circ$ |
| 4C 34.47 | 1996 Jun | 2 | $0.94 \pm 0.09\%$ | $146^\circ \pm 3^\circ$ |
| | 1998 May | 1 | $1.13 \pm 0.15\%$ | $146^\circ \pm 4^\circ$ |
| | 1998 Sep | 3 | $0.99 \pm 0.10\%$ | $149^\circ \pm 3^\circ$ |
| | 1998 Nov | 1 | $0.87 \pm 0.15\%$ | $141^\circ \pm 5^\circ$ |
| | 1999 May | 1 | $0.89 \pm 0.09\%$ | $149^\circ \pm 3^\circ$ |
| 4C 09.72 | 1996 Dec | 12 | $1.32 \pm 0.04\%$ | $118^\circ \pm 2^\circ$ |
| | 1997 Dec | 3 | $1.36 \pm 0.11\%$ | $112^\circ \pm 3^\circ$ |
| | 1998 Nov | 1 | $1.23 \pm 0.19\%$ | $117^\circ \pm 5^\circ$ |

[a]Number of observations.

[b]Summed over a broad continuum interval near the middle of the observed spectrum.

[c]"White-light" ($\lambda\lambda 3200 - 8600$) measurement obtained with a filter polarimeter.

Table 3
Optical Polarization and Radio Structure

| Quasar | $P_{\rm opt}$ (%) | $\theta_{\rm opt}$ | Radio Axis[1] (as; mas) | $\theta_{\rm opt} - \theta_{\rm rad}$ |
|---|---|---|---|---|
| 3C 95 | 0.82 | 176° | 164°; ··· | 12° |
| PKS 0405−12 | 0.27 | 124° | 12°; 170°: | −68° |
| B2 1208+32 | 1.04 | 18° | 3°; ··· | 15° |
| Ton 202 | 1.74 | 68° | 53°; ··· | 15° |
| 4C 37.43 | 1.24 | 100° | 109°; ··· | −9° |
| 3C 323.1 | 1.47 | 22° | 20°; ··· | 2° |
| 4C 34.47 | 0.95 | 148° | 162°; 167° | −14° |
| 4C 09.72 | 1.32 | 117° | 145°; ··· | −28° |

[1]References for radio structure — 3C 95: Price et al. 1993; PKS 0405−12: Fanti et al. 1977, Rusk & Seaquist 1985; B2 1208+32: Fanti et al. 1977; Ton 202, 4C 37.43, 3C 323.1, & 4C 09.72: Kellerman et al. 1994; 4C 34.47: Barthel et al. 1989

Table 4
Characteristics of the Polarized Spectra

| Quasar | $\alpha$[a](±∼0.2) | $f_p$[b] |
|---|---|---|
| 3C 95 | −1.1 | 0.8 |
| B2 1208+32 | −1.0 | 1.0 |
| Ton 202 | −0.8 | 0.8 |
| 4C 37.43 | −0.8 | 1.2 |
| 3C 323.1 | −0.9 | 0.6 |
| 4C 34.47 | +0.1 | 0.4 |
| 4C 09.72 | −0.8 | 1.5 |

[a]Spectral index of polarized flux $\alpha = d\log(q' \times F_\nu)/d\log\nu$

[b]$3\sigma$ upper limit to the flux fraction of the strongest broad emission line that could share the polarization of the continuum.

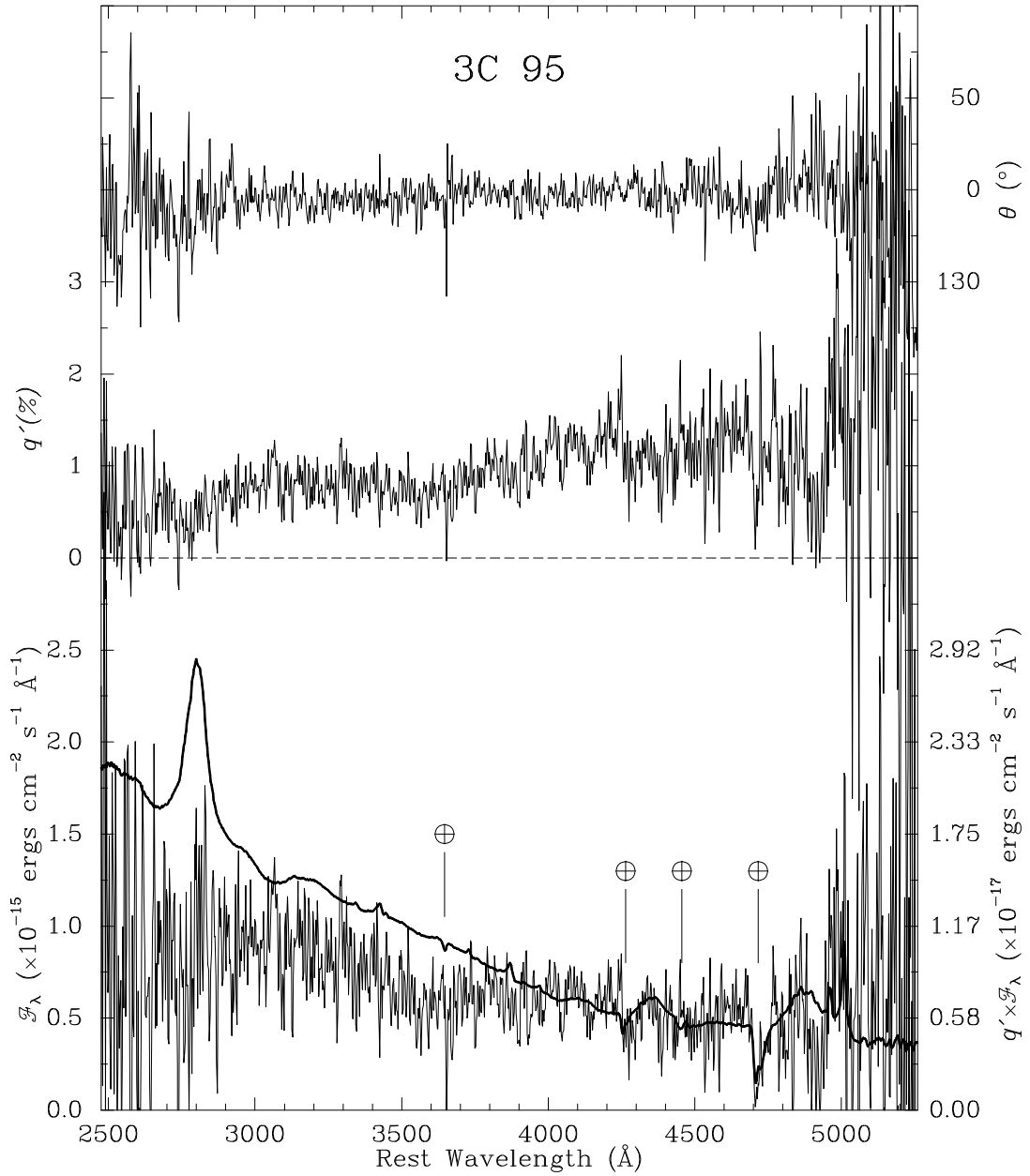


FIG. 1.— Spectropolarimetry summed over all epochs for 3C 95. *Bottom panel:* Total flux spectrum (bold line and left ordinate) and polarized flux $q' \times F_\lambda$ (thin line and right ordinate), normalized at long wavelengths. *Middle panel:* Stokes parameter $q'(\%)$ for a coordinate system rotated to the systemic position angle of polarization. *Top panel:* Position angle of polarization in degrees. Note depressions in the degree of polarization in the "3000 Å bump" and at each major emission line, and the corresponding smoothly rising polarized flux spectrum. Artifacts caused by strong terrestrial absorption and emission features are marked.

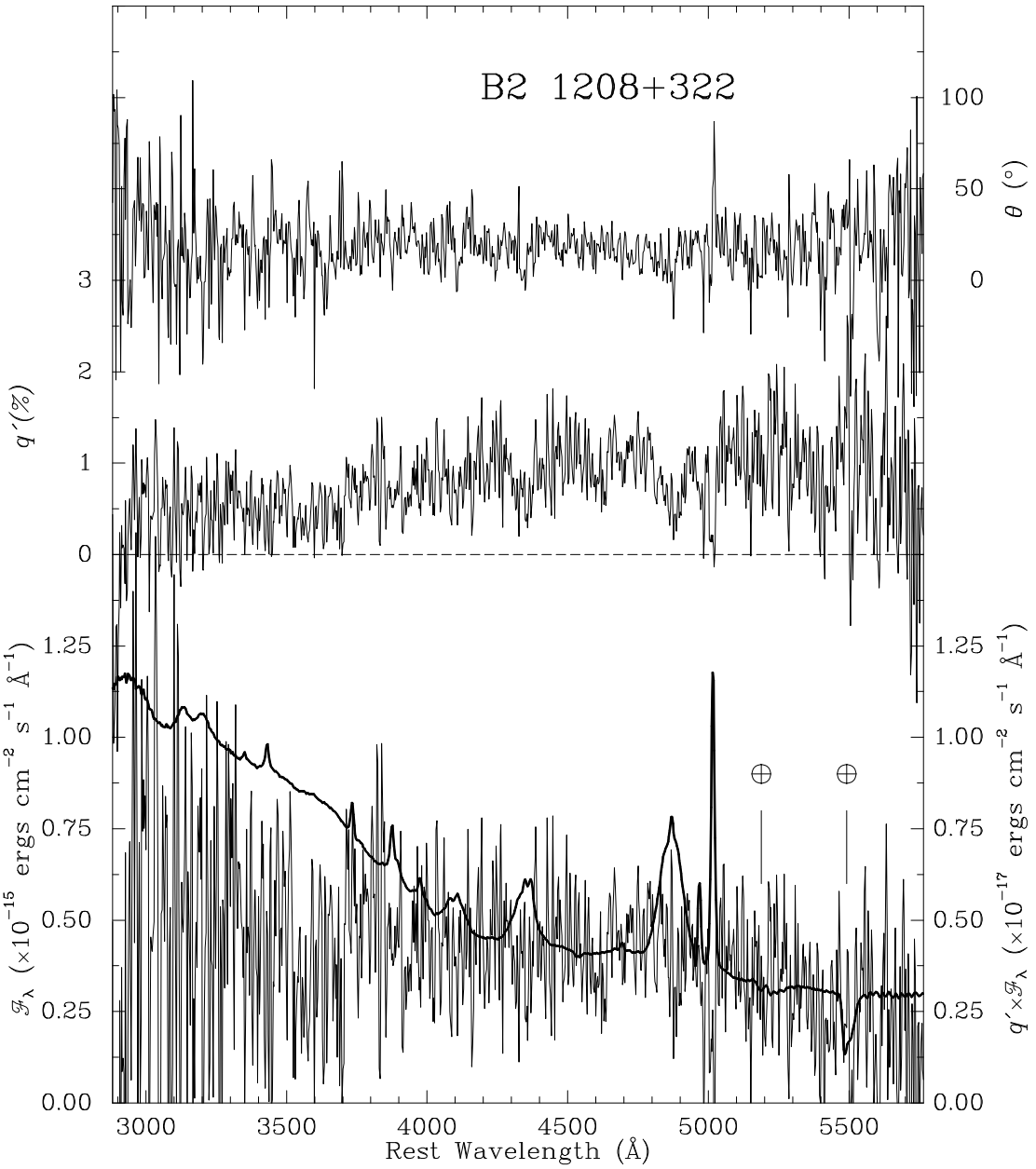


FIG. 2.— As in Fig. 1 for B2 1208+322.

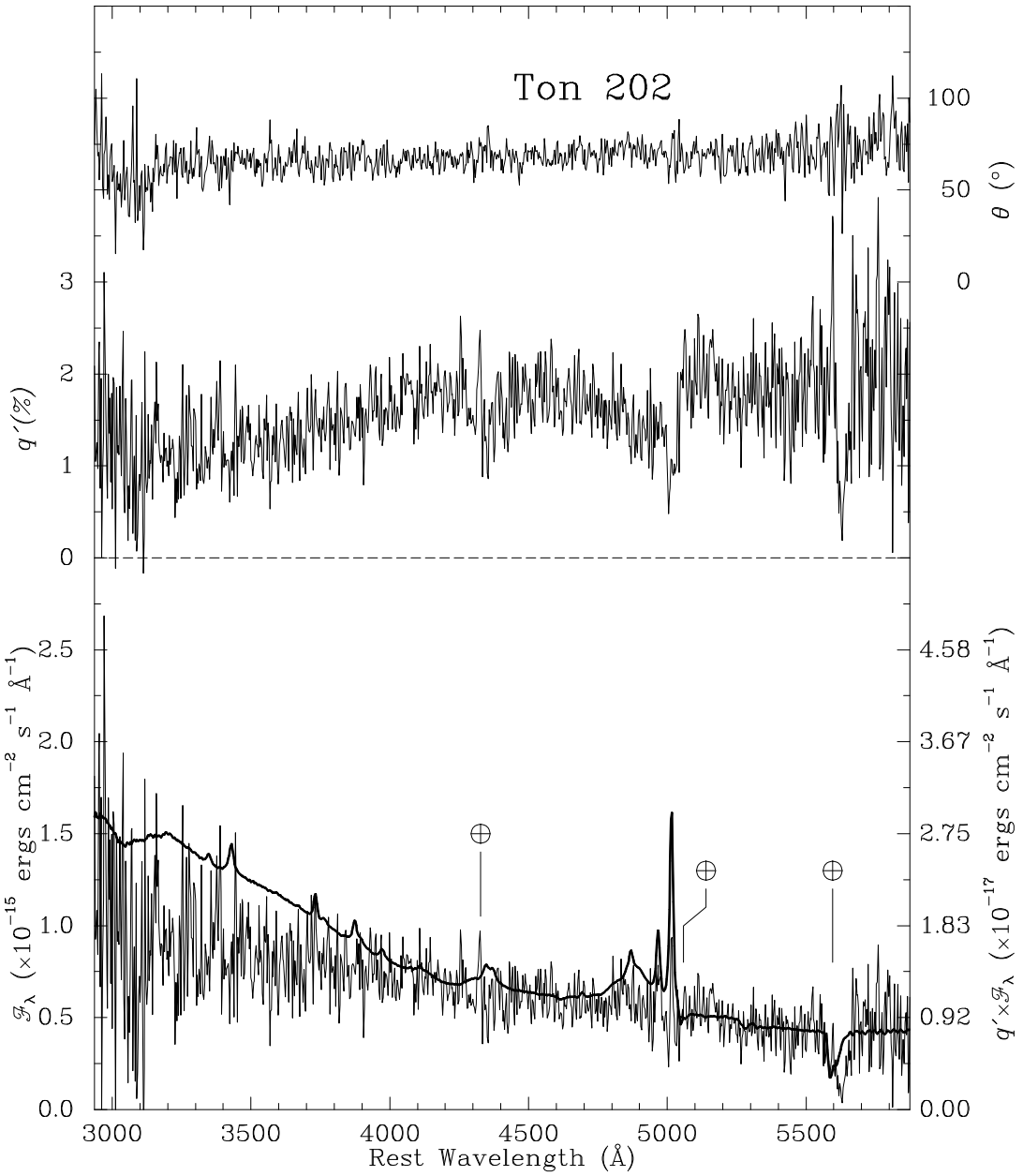


FIG. 3.— As in Fig. 1 for Ton 202.

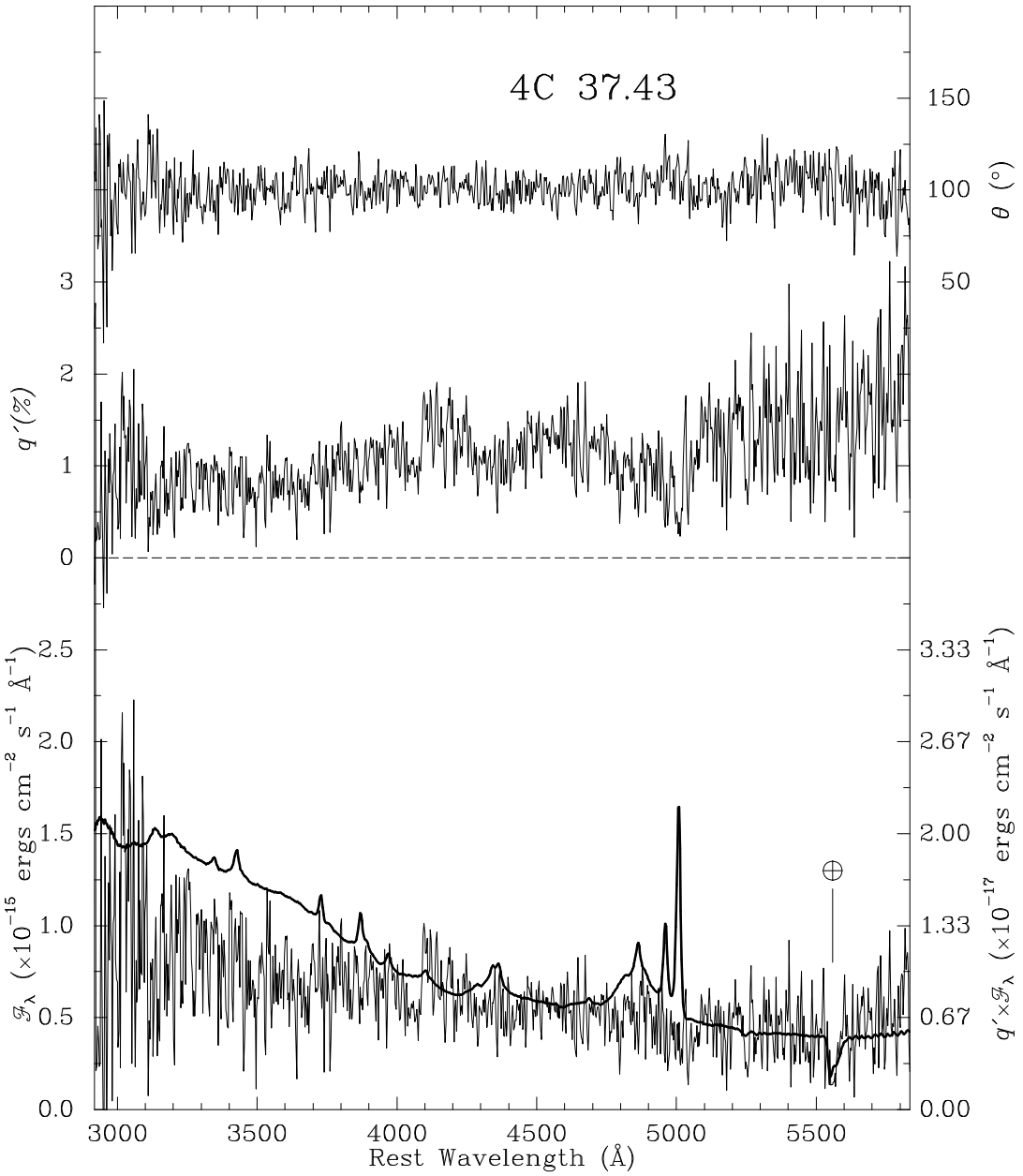


FIG. 4.— As in Fig. 1 for 4C 37.43.

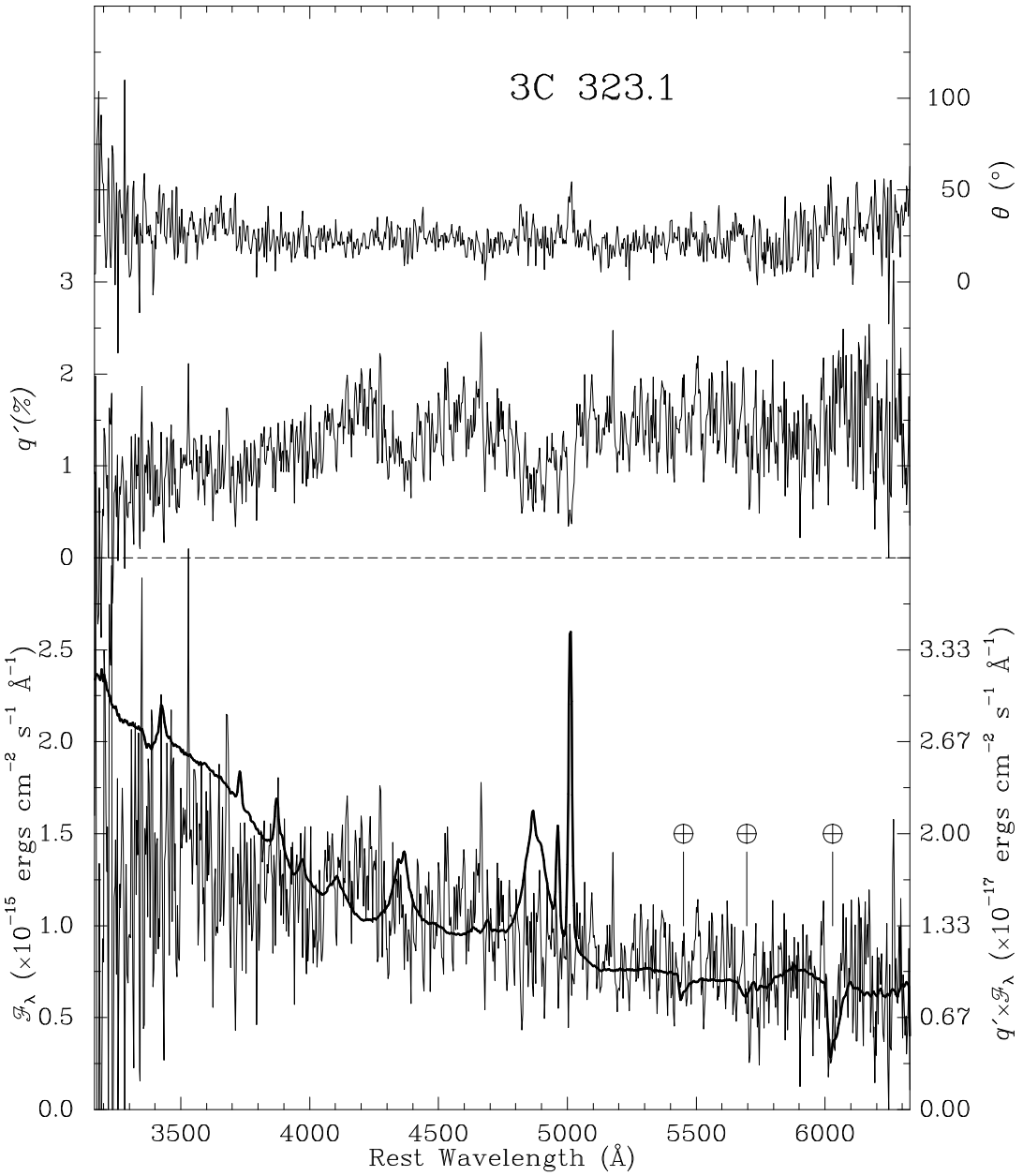


FIG. 5.— As in Fig. 1 for 3C 323.1.

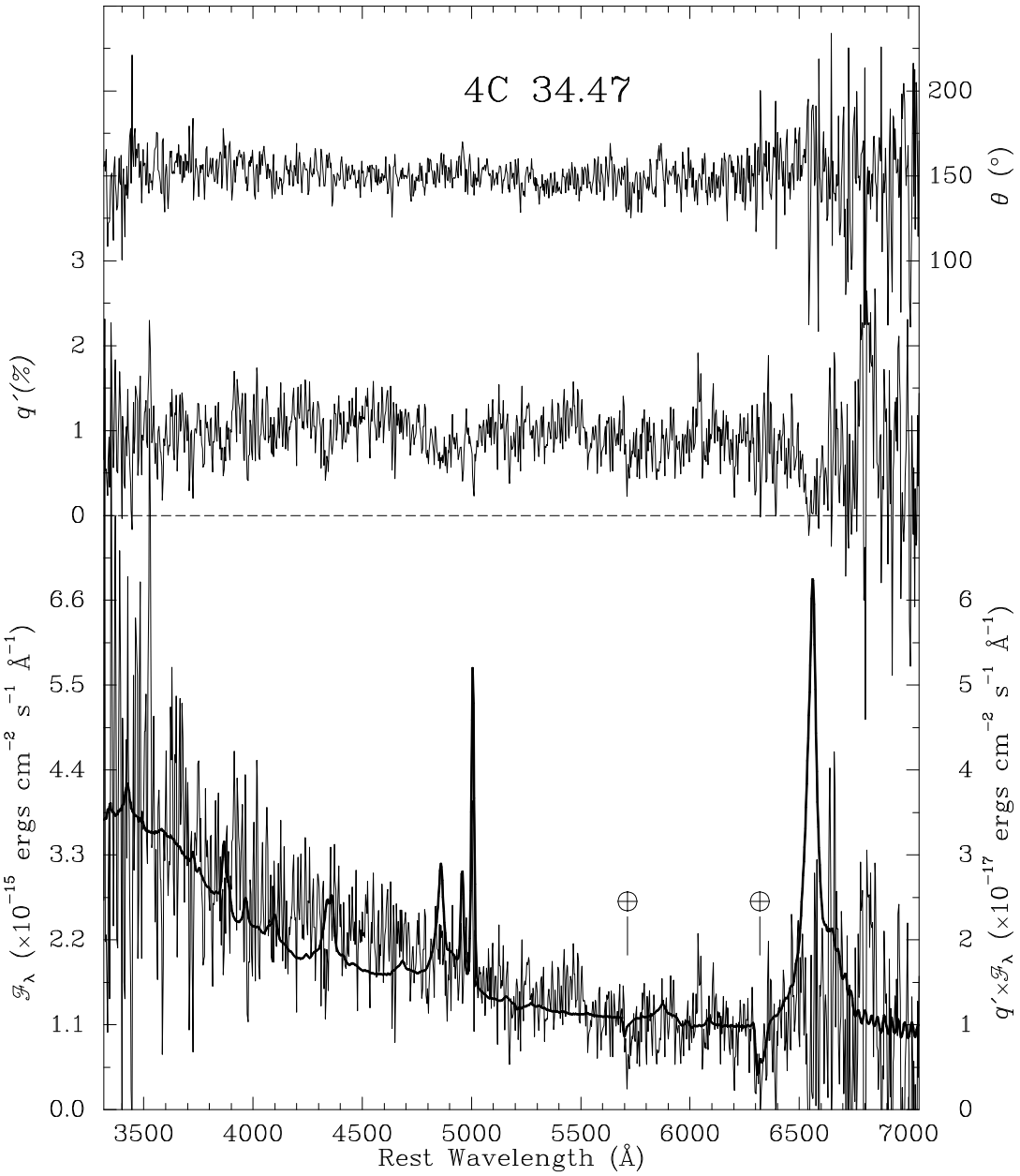


FIG. 6.— As in Fig. 1 for 4C 34.47.

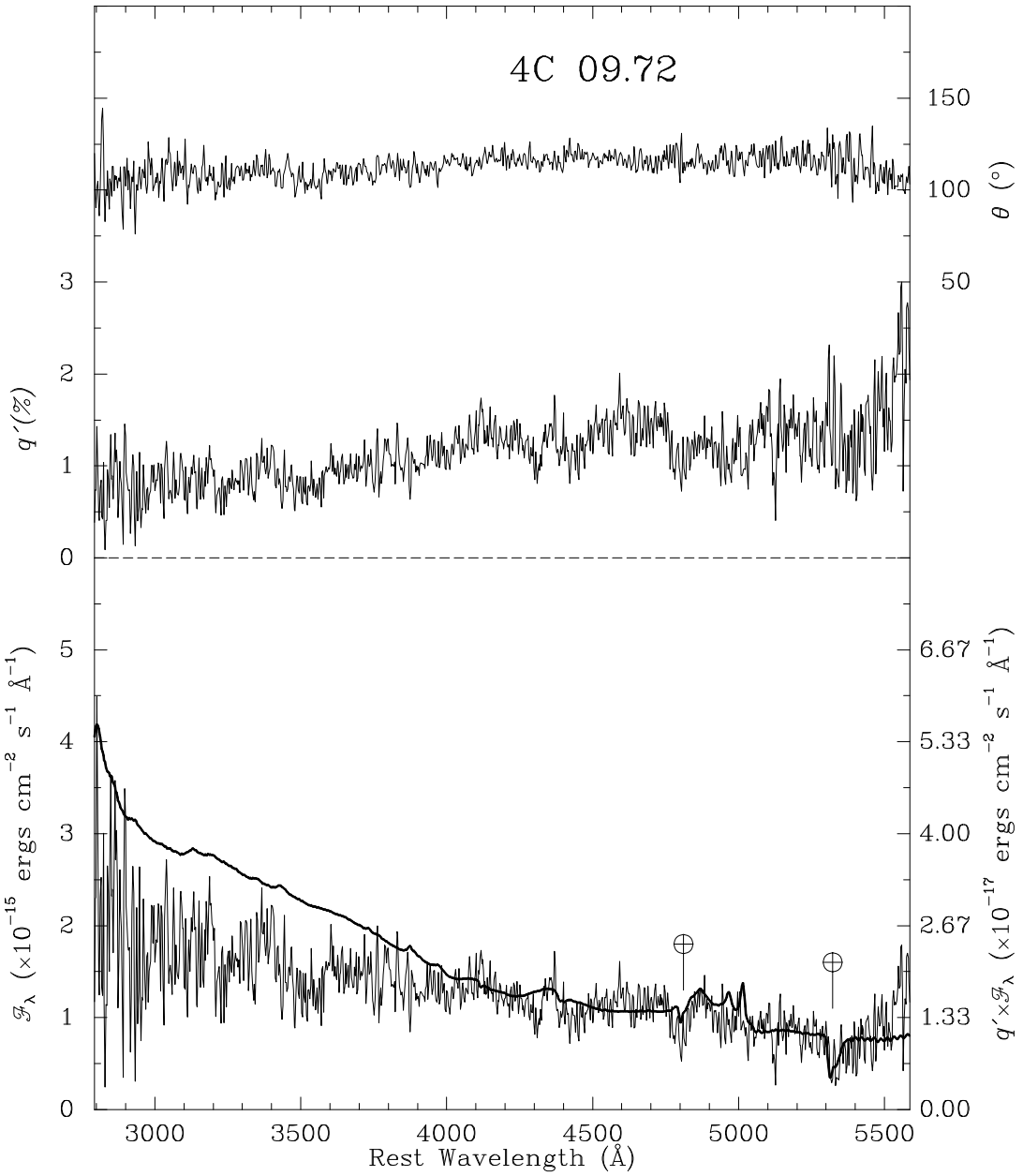


FIG. 7.— As in Fig. 1 for 4C 09.72.